J. Membrane Biol. 173, 39–46 (2000)

The Journal of
Membrane
Biology



# Regulation of Lens rCx46-formed Hemichannels by Activation of Protein Kinase C, External $Ca^{2+}$ and Protons

**B. Jedamzik[1], I. Marten[1], A. Ngezahayo[1], A. Ernst[2], H.-A. Kolb[1]**

[1]Institut für Biophysik, Universität Hannover, Herrenhäuserstr. 2, D-30419 Hannover, Germany
[2]HNO-Klinik, UKB Berlin, Rapsweg 55, D-12683 Berlin, Germany

Received: 30 March 1999/Revised: 18 September 1999

**Abstract.** Rodent lens connexin46 (rCx46) formed active voltage-dependent hemichannels when expressed in *Xenopus* oocytes. Time-dependent macroscopic currents were evoked upon depolarization. The observed two activation time constants were weakly voltage-dependent and in the order of hundreds of milliseconds and seconds, respectively. Occasionally, the macroscopic steady-state current and the corresponding current-voltage curve showed inactivation at high depolarizing voltages (>+50 mV). To account for the fast recovery from inactivation (<2 msec) favored by hyperpolarization, a four-state kinetic model ($C_{1closed} \leftrightarrow C_{2closed} \leftrightarrow O_{open} \leftrightarrow I_{inactivated}$) is proposed. In the absence of inactivation, the macroscopic conductance decreased and inactivation became visible at voltages positive of +50 mV when the rCx46-expressing oocytes were treated with the protein-kinase-C-activators OAG or TPA, high external concentrations of $Ca^{2+}$ or $H^+$. However, the underlying mechanisms of OAG, $H^+$ or $Ca^{2+}$ action were different. While OAG did not alter the voltage-dependent activation of the rCx46-hemichannels, an increase in the external $Ca^{2+}$ or $H^+$ level shifted the voltage threshold for activation to more positive voltages. In contrast to $Ca^{2+}$, protons were not effective in the physiological concentration range. We propose that under physiological conditions only external $Ca^{2+}$ and intracellular PKC-dependent processes regulate rCx46 in the lens.

**Key words:** $Ca^{2+}$ — Connexin46 — Hemichannel activation — Inactivation — pH — OAG/TPA

## Introduction

Gap junction channels are the intercellular bridges allowing the cytoplasmic transport of ions and small molecules between neighboring animal cells. One gap junction channel consists of two connexons (hemichannels) each located in the plasma membrane of the opposed cells. At the molecular level, connexons are composed of six polypeptides, the connexins. So far, at least 13 different connexins have been cloned in rodents (Bruzzone, White & Paul, 1996). Most tissues express more than one type of connexin (Cx). Four different types such as Cx44, Cx46, Cx50, Cx56 are found in the lens (Paul et al., 1991; Rup, 1993; Gupta et al., 1994; Lin et al., 1998). Since the lens is an avascular tissue, its vitality and function depend highly on proper cell-cell coupling. The gap junction channels very likely provide the basis for sharing ions, second messengers and metabolites between lens cells located near the aqueous/vitreous humor and the core region (Mathias et al., 1997). For a better understanding of the physiology of the lens, it is of crucial importance to study how this tissue regulates its gap junctional coupling.

In the lens, the gap junction channels in the cortical region are sensitive to internal pH, but the gap junction channels in the core region are not pH sensitive (Mathias et al., 1991; Baldo & Mathias, 1992; Lin et al., 1998). It is also known that due to bacterial infection the pH of the vitreous humor can decrease from 7.4 to 6.6 (Davey, Barza & Peckman, 1987). The pH sensitivity in the cortical region may represent a mechanism developed by the lens for self-insulation when the vitreous humor becomes infected. However, the insensitivity of the core region to acidification may represent an adaptation to the low pH measured in this region of the lens. This feature allows cell-cell coupling even at a reduced pH (lens cortex: pH 7.4 *vs.* lens core: pH 6.8; Bassnet & Duncan, 1985). The internal pH insensitivity may be due to post-translational modification of the gap junction channels in the core region of the lens that results in a truncated C-terminus and in turn loss of pH susceptibility (Lin et al., 1998).

Further insights in the function of gap junction chan-

*Correspondence to:* H.-A. Kolb

nels from the lens were obtained on the basis of their individual hemichannels (Cx46, Cx56) that do form active connexons in the expression system *Xenopus laevis* oocytes (Paul et al., 1991; Ebihara & Steiner, 1993; Gupta et al., 1994; Ebihara, Berthoud & Beyer, 1995). The voltage-dependent properties of the rCx46- or chicken Cx56-formed hemichannels reflected those of the corresponding gap junction channels (Ebihara et al., 1995). Ebihara and Steiner (1993) also demonstrated that the gating behavior of rCx46-hemichannel depends on the external $Ca^{2+}$ concentration. Recently, we showed that activation or inhibition of protein kinase C (PKC) influenced the conductance of the rCx46-hemichannels (Ngezahayo et al., 1998), suggesting that phosphorylation/dephosphorylation processes most likely contribute to rCx46-hemichannel regulation.

Since (i) the pH varies in different regions of the lens or decreases during bacterial infection (Bassnet & Duncan, 1985; Davey et al., 1987), and (ii) evidence was provided that hemichannel activation might occur in native tissues (DeVries & Schwarz, 1992; Malchow et al., 1994), we examined the dependence of the rCx46-hemichannel activity on external pH in comparison to external $Ca^{2+}$ and PKC activation. The results show that external pH, pCa and the PKC-activators OAG or TPA differentially altered the activation and inactivation behavior of the rCx46-hemichannels. We suggest that phosphorylation/dephosphorylation processes and external $Ca^{2+}$ ions rather than the external pH are involved in controlling the activity of hemichannels under physiological conditions.

## Material and Methods

### Molecular Biology

*Xenopus laevis* oocytes were prepared and injected with rCx46-encoding RNA, as described by Ngezahayo et al. (1998).

### Electrophysiological Measurements

Recordings of macroscopic currents were performed from single *Xenopus* oocytes 1–2 days after RNA injection at room temperature. Currents were recorded using a voltage-clamp amplifier Turbo TEC-10 CD (npi electronic, Tamm, Germany). Voltage protocols were applied by a Pentium 100 MHz Computer linked to an ITC-16 interface (Instrutech, NY). The following pulse protocol was used throughout the experiments. From a constant holding voltage of −90 mV test potentials were applied for 10 sec in the range from −110 mV to +70 in 15 mV-increments. Repolarization occurred at the holding voltage $V_H$ = −90 mV which was kept for at least 10 sec. Currents were filtered at 1 kHz and were sampled at 0.5 or 0.25 kHz. Data acquisition and analysis were performed by using Pulse/PulseFit (HEKA, Germany), Igor Pro (Wave Metrics, USA), Excel (Microsoft), PatchMaschine (V. Avdonin, University of Iowa, IA) and MeinSweeper (B. Jedamzik, University of Hannover, Germany). *n* denotes the numbers of individual experiments (= oocytes). Errors represent the standard deviation of the sample (SD).

### Data Analysis

The steady-state current amplitudes $I_{ss}$ were leak-subtracted and shown as function of the ion driving force ($V - V_{rev}$) in Figs. 2*A* and 3*B*. Leak currents were determined by extrapolation of the corresponding data points between −110 to −65 mV and the reversal potential ($V_{rev}$) by linear regression. The reversal potential ($V_{rev}$) of the non-leak-subtracted $I_{ss}(V)$ curve was calculated by an 4-point interpolation polynom.

The macroscopic conductance was calculated from the steady-state current amplitude under consideration of the ion driving force ($V - V_{rev}$). The derived values were plotted as a function of the test potential. To describe at steady-state the voltage-dependent conductance without significant influence of inactivation, the corresponding current values measured in the range from −110 to +40 mV were considered and fitted with a simple Boltzmann distribution as given by the following function: $G(V) = (A/(1 + \exp(-(V - V_{1/2})zF/RT) + B)$. *R, T, F* have their usual meanings, $V_{1/2}$ represents the half-activation voltage at which 50% of the maximal conductance is reached, *z* represents the number of apparent equivalent gating charges. The parameter *A* gives the maximal macroscopic conductance of the hemichannels, *B* represents the nonvoltage-dependent leak conductance. The $G(V)$ curves were normalized to the derived fits by setting $A = 1$ and $B = 0$.

The theoretical values shown in Fig. 1*D* ($I_{ss}'$, open symbols) were calculated by the following equation: $I_{ss}'(V - V_{rev}) = (V - V_{rev}) \cdot I_{tail}/(V_H - V_{rev})$ where $I_{tail}$ gives the instantaneous tail current amplitude recorded at the holding voltage $V_H$ after application of the test potential *V*.

### Solutions

Voltage- and current-recording micropipettes were filled with 3 M KCl and had an input resistance of 1–1.5 MΩ. The control bath solution was nominally $Ca^{2+}$-free and contained 100 mM KCl, 2 mM $MgCl_2$, 10 mM MES/TRIS (pH 7.7). The osmolality of all bath solutions was adjusted to 240 mosmol/kg with D-sorbitol. A stock solution of 200 mM OAG (1-oleoyl-2-acetyl-*sn*-glycerol; Calbiochem-Novabiochem GmbH, Bad Soden, Germany) was prepared by dissolving OAG in DMSO (Merck, Darmstadt, Germany). Using the control bath solution, the OAG/DMSO-stock solution was diluted to the final concentration of 200 μM and 0.25% DMSO just before the beginning of experimentation. TPA (phorbol-12-myristate-13-acetate; Calbiochem-Novabiochem GmbH, Bad Soden, Germany) was dissolved in DMSO and diluted in the control bath solution to a final concentration of 1 nM TPA and 0.25% DMSO. The control bath solution which were used as a reference for the OAG and TPA experiments additionally contained 0.25% DMSO. During the current recordings the oocytes were continuously perfused at a rate of 0.5 ml/min. The experiments were performed at room temperature.

## Results

### Voltage-Dependent Activation and Inactivation of rCx46-Hemichannels

Representative voltage-jump current-relaxations were recorded from rCx46-expressing *Xenopus laevis* oocytes under control bath conditions (Fig. 1*A* and *B*). To enable voltage-dependent activation of the rCx46-hemichannels, the oocytes were bathed in a 'pseudo-intracellular' solution containing a high $K^+$ and a low $Ca^{2+}$ concentration (Ebihara et al., 1995). Test potentials

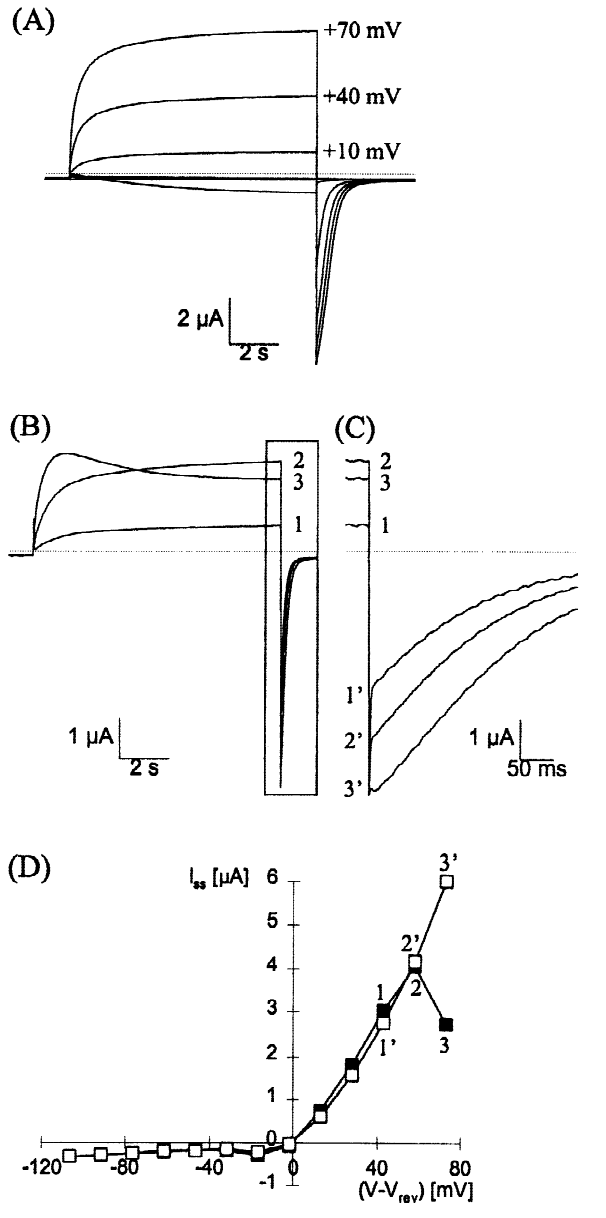


**Fig. 1.** Voltage-dependent hemichannel activation and inactivation with fast recovery. (*A*) Representative voltage-dependent current relaxation. Note the absence of a spontaneously occurring current inactivation at high depolarizing voltages. For clearer presentation, current traces evoked by voltage steps to −110, −80, −50, −20, +10, +40, +70 mV were only shown. The dashed line represents the zero current level. (*B*) Representative current traces evoked by voltage steps to +40 mV (1), +55 mV (2) and +70 mV (3). Following a transient rise, the current amplitude spontaneously decreased at a depolarizing voltage step to +70 mV (3) reflecting hemichannel inactivation. (*C*) Raw current traces from (*B*) are shown with a higher time resolution. Note that the inactivation-induced decrease in the steady-state current amplitude at +70 mV (3) is not seen in the corresponding instantaneous tail current amplitude (3′). (*D*) The non-leak subtracted steady-state current amplitudes ($I_{ss}$, ■) from (*B*) are plotted as a function of the ion driving force ($V - V_{rev}$) showing the inactivation behavior at +70 mV (3). For comparison, the instantaneous tail current amplitudes were used to determine the theoretical steady-state current amplitudes ($I_{ss}'$, □). Note that the theoretical value at +70 mV (3′) did not reflect the inactivation behavior of the corresponding steady-state current amplitude (3).

applied in the range from −110 to +70 mV from a constant holding potential of −90 mV often induced current responses without visible inactivation (Fig. 1*A*). However, as indicated by the current decline following a transient rise in the outward current amplitude (Fig. 1*B*), the rCx46-hemichannels occasionally showed inactivation at test potentials more positive than +50 mV. The magnitude of inactivation remained stable throughout the course of an experiment (up to 180 min). Further, current inactivation was incomplete still leaving a large fraction of the outward current amplitude at the end of the long-lasting voltage pulse (Fig. 1*B*). The steady-state current-voltage relationship ($I_{ss}(V - V_{rev})$) derived from spontaneously inactivating hemichannels is shown in Fig. 1*D*. Despite the increasing ion driving force, the steady-state current amplitude at +70 mV was lower than that measured at +55 mV indicating an inactivation behavior of the hemichannels (closed squares 2 *vs.* 3 in Fig. 1*D*). However, the instantaneous tail current amplitudes evoked upon hyperpolarization did not reflect this inactivation behavior observed at the preceding voltage pulse to +70 mV (*cf.* 3 with 3′ in Fig. 1*B–D*). Thus, recovery from inactivation occurred several orders of magnitude faster (<2 msec) than deactivation.

To describe the voltage-dependent steady-state activation of the rCx46-hemichannels, macroscopic conductance-voltage ($G(V)$) curves were determined in the absence of visible inactivation (*see* Fig. 1*A*). The $G(V)$ curves show that the hemichannels stayed in the closed state at test potentials more negative than −65 mV but opened at depolarizing potentials (Table 1, Figs. 2*B*, 3*C–D*). A half-maximal voltage activation $V_{1/2} \approx -30$ mV and a number of apparent equivalent gating charges $z \approx 3$ were derived by fitting the $G(V)$ curves with a simple Boltzmann function under control conditions. The time course of activation was characterized by at least two activation time constants. The fast activation time constant was about 250 msec in the range from +15 to +55 mV ($\tau_{+15mV} = 256.2 \pm 37.4$ msec, $n = 27$; $\tau_{+55mV} = 232.1 \pm 29.0$ msec, $n = 23$) indicating no significant voltage dependence. The slow activation time constants were in the order of seconds ($\tau_{+15mV} = 2.1 \pm 0.4$ sec, $n = 27$; $\tau_{+55mV} = 3.4 \pm 1.0$ sec, $n = 23$).

## The Effect of External $Ca^{2+}$ on the Voltage-Dependent Membrane Conductance

A rise in the external $Ca^{2+}$ concentration from nominal $Ca^{2+}$-free (control bath solution) to the millimolar range was found to suppress the voltage-stimulated current amplitude of rCx46-hemichannels (Fig. 2*A; see also* Ebihara & Steiner, 1993). To study the $Ca^{2+}$ effect, we only used rCx46-expressing oocytes showing no current inactivation at +70 mV under control conditions. The steady-state current-voltage relation ($I_{ss}(V - V_{rev})$) obtained under nominal $Ca^{2+}$-free conditions (control bath solution) and in the presence of 1 mM $Ca^{2+}$ were plotted in Fig. 2*A*. Compared to the control, the steady-state current ampli-

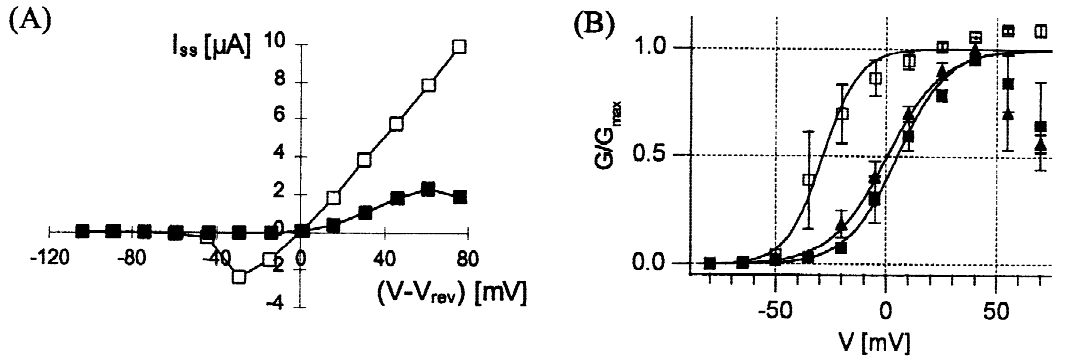


**Fig. 2.** Voltage dependence of macroscopic rCx46-currents and corresponding membrane conductance at different $Ca^{2+}$ concentrations in the bath. (*A*) Current-voltage relation ($I_{ss}(V - V_{rev})$) derived from a typical oocyte in nominal $Ca^{2+}$-free control bath solution (□) does not show current inactivation but do after addition of 1 mM $Ca^{2+}$ to the bath (■). (*B*) Normalized voltage-dependent membrane conductance ($G(V)/G_{max}$) were determined for nominal $Ca^{2+}$-free bath solution (□, $n = 7$) or for bath solution containing 0.5 mM $Ca^{2+}$ (▲, $n = 4$) and 1 mM $Ca^{2+}$ (■, $n = 5$). The solid lines represent fits of the data points with a simple Boltzmann function (for details *see* Materials and Methods). To exchange the bath solution within less than 2 min, the perfusion rate was increased to 2 ml/min.

tude was reduced in 1 mM $Ca^{2+}$ over the whole voltage range. The $G(V)$ curves showed that the half-maximal activation voltage $V_{1/2}$ shifted by about +30 mV to depolarizing voltages with increasing extracellular $Ca^{2+}$ levels (Fig. 2*B*, Table; Ebihara & Steiner, 1993). This $Ca^{2+}$-induced shift of the voltage threshold for hemichannel activation likely caused the reduction in the current amplitude (Fig. 2*A*). Furthermore, the comparison of the number of equivalent gating charges $z$ revealed a decrease from $z = 3.2$ to about $z = 2.0$ (Table). The significance of the $Ca^{2+}$ effect was examined by applying the unpaired *t*-test for determination of the $P$ value (Table). On the basis of the *t*-test, the change in $V_{1/2}$ but not in $z$ was statistically significant (e.g., at 1 mM $Ca^{2+}$: $P_{V1/2} < 0.0001$; $P_z = 0.0582$). As observed for the spontaneously occurring inactivation (Fig. 1*B–D*), the outward current amplitude at +70 mV was lower than the current amplitude at +55 mV. In line with this observation, the $G(V)$ curve at high external $Ca^{2+}$ showed a decline in the conductance above +50 mV (Fig. 2*B*) indicating that hemichannel inactivation became visible at highly depolarized voltages in the presence of high external $Ca^{2+}$. However, as found for the spontaneously occurring inactivation under control conditions (nominal free $Ca^{2+}$; Fig. 1), the current decrease at +70 mV in the presence of $Ca^{2+}$ (1 mM) was not observed in the corresponding instantaneous tail current amplitude.

### The Effect of External $H^+$ on the Voltage-Dependent Membrane Conductance

Since the lens regions (core, cortex) are characterized by different pH (Bassnet & Duncan, 1985), the effect of external protons on the gating of rCx46-hemichannels were examined. A change in the external pH from 7.7 to 8.8 and to 6.6 did not significantly alter the current response of voltage-stimulated rCx46-expressing oocytes (Fig. 3*A* and *B*). As demonstrated by the corresponding current-voltage curves ($I_{ss}(V - V_{rev})$), compared to pH 7.7, the current amplitude $I_{ss}$ at +70 mV was only slightly increased or reduced at pH 8.8 and pH 6.6, respectively (Fig. 3*A* and *B;* pH 6.6 *not shown*). In line with this observation, the $G(V)$ curves obtained for pH 8.8, pH 7.7 and pH 6.6 were similar (Fig. 3*C*). However, as at high external $Ca^{2+}$ (Fig. 2; *see also* Ebihara & Steiner, 1993), further external acidification from pH 7.7 to 6.0 reversibly suppressed the voltage-evoked current amplitude (Fig. 3*A* and *B*) and increased the fast activation time constants (e.g., at +40 mV: $\tau_{pH7.7} = 265.3 \pm 0.04$ msec, $\tau_{pH6.0} = 540.8 \pm 0.08$ msec; $n = 3$). Previous studies reported that internal acidification reduced the gap junctional conductance (Ek et al., 1994). We observed that external pH at 6.0 affected the conductance of rCx46-hemichannels faster than internal acidification altered the gap junction conductance of paired hemichannels (Ek et al., 1994). Thus, we conclude that the effects on rCx46-hemichannels seen at an external pH of 6.0 resulted from a change in the external rather than in the internal pH. Acidification to pH 6.0 also shifted the $G(V)$ curve by about +25 mV to more positive voltages ($P = 0.0002$) causing the observed reduction of the current amplitude (Fig. 3*A, B, D;* Table). An external pH of 6.0 decreased the number of equivalent gating charges $z$ by about 47% ($z_{pH6.0} = 1.66 \pm 0.16$, $n = 6$; $z_{pH7.7} = 3.03 \pm 0.82$, $n = 7$; $P = 0.0021$; Table). Additionally, the $G(V)$ curve for pH 6.0 revealed decreasing conductance at voltages >+50 mV. Like at high external $Ca^{2+}$ or with spontaneously occurring inactivation, the decline in current or macroscopic conductance was not reflected by the instantaneous tail current amplitude recorded at the holding voltage (not shown, *cf.* Fig. 1*B–D*). This observation indicates that hemichannel inactivation became visible at high external acidification.

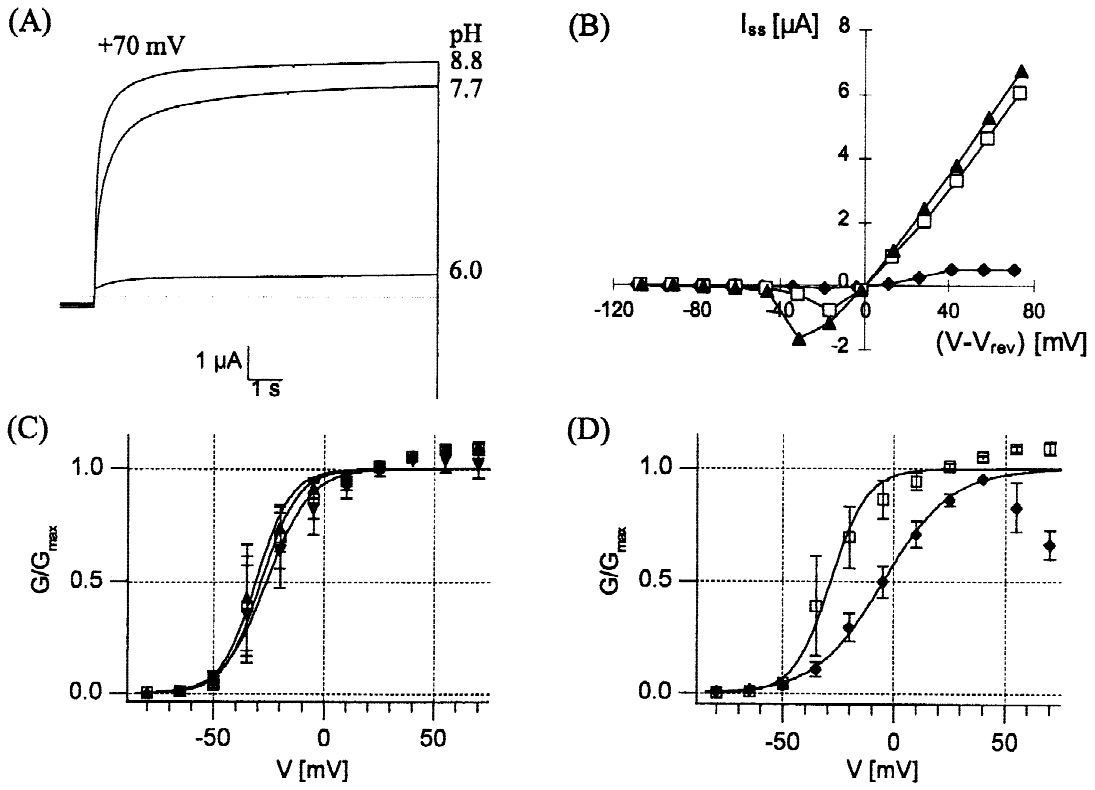


**Fig. 3.** Effect of external pH on voltage-dependent currents and conductance in the absence of spontaneously occurring inactivation. (*A*) Current relaxations were recorded at different pH as indicated. For clearer presentation only the current responses evoked by a voltage step to +70 mV are given. (*B*) Current-voltage ($I_{ss}(V - V_{rev})$) relations obtained with pH 8.8 (▲), 7.7 (□) and 6.0 (◆) in the bath solution are presented. (*C*) Normalized $G(V)$ curves were determined for control bath solution at pH 7.7 (□, $n = 7$), pH 8.8 (▲, $n = 4$) and pH 6.6 (▼, $n = 6$). (*D*) Normalized $G(V)$ curves were obtained for control bath solution at pH 7.7 (□, $n = 7$; *see also C*) and pH 6.0 (◆, $n = 6$). Data points in *C* and *D* were fitted with a simple Boltzmann function (solid lines). To change the bath solution within less than 2 min, the perfusion rate was increased to 2 ml/min.

**Table 1.** Effect of OAG, external $Ca^{2+}$ and $H^+$ on the voltage-dependent properties of rCx46-hemichannels

| pH | DMSO [%] | $Ca^{2+}$ [mM] | OAG [mM] | $V_{1/2}$ [mV] | $z$ | $n$ | $P$ value for $V_{1/2}$ | $P$ values for $z$ |
|---|---|---|---|---|---|---|---|---|
| 8.8 | — | — | — | −30.9 ± 7.5 | 3.17 ± 0.28 | 4 | 0.6562 | 0.7492 |
| *7.7 | — | — | — | −28.5 ± 8.8 | 3.03 ± 0.28 | 7 | — | — |
| 6.6 | — | — | — | −26.1 ± 10.1 | 2.58 ± 0.38 | 6 | 0.6485 | 0.2911 |
| 6.0 | — | — | — | −4.8 ± 5.8 | 1.66 ± 0.16 | 6 | 0.0002 | 0.0021 |
| 7.7 | — | 0.5 | — | 0.5 ± 2.8 | 1.98 ± 0.19 | 4 | 0.0001 | 0.0359 |
| 7.7 | — | 1.0 | — | 5.1 ± 4.8 | 2.22 ± 0.17 | 5 | <0.0001 | 0.0582 |
| *7.7 | 0.25 | — | — | −22.3 ± 10.1 | 2.56 ± 0.30 | 10 | — | — |
| 7.7 | 0.25 | — | 0.2 | −16.1 ± 6.7 | 2.45 ± 0.50 | 10 | 0.1225 | 0.5696 |

Half-activation voltages $V_{1/2}$ and the number of equivalent gating charges $z$ obtained upon fitting macroscopic conductance-voltage curves with a simple Boltzmann function are used to describe the voltage-dependent steady-state activation of rCx46-hemichannels. To examine the significance of the OAG-, $Ca^{2+}$- and $H^+$-effect, the parameters were statistically compared with those obtained under control conditions (*see* asterisk-labeled rows; control for $Ca^{2+}$ and pH: upper-marked row; control for OAG: lower-marked row) by using an unpaired *t*-test (*P*-value).

## The Effect of the Protein Kinase C Activator OAG on the Voltage-Dependent Membrane Conductance

Recently, Ngezahayo et al. (1998) reported that the protein-kinase-C activator OAG reduced the macroscopic conductance and induced a visible inactivation behavior of the hemichannels when current inactivation did not occur spontaneously (Fig. 4*A*). Similar results were obtained when rCx46-expressing oocytes were superfused with 1 nM TPA, a well-known PKC-activator (Fig. 4*C*). Like OAG (Fig. 4*A*), TPA decreased the current ampli-

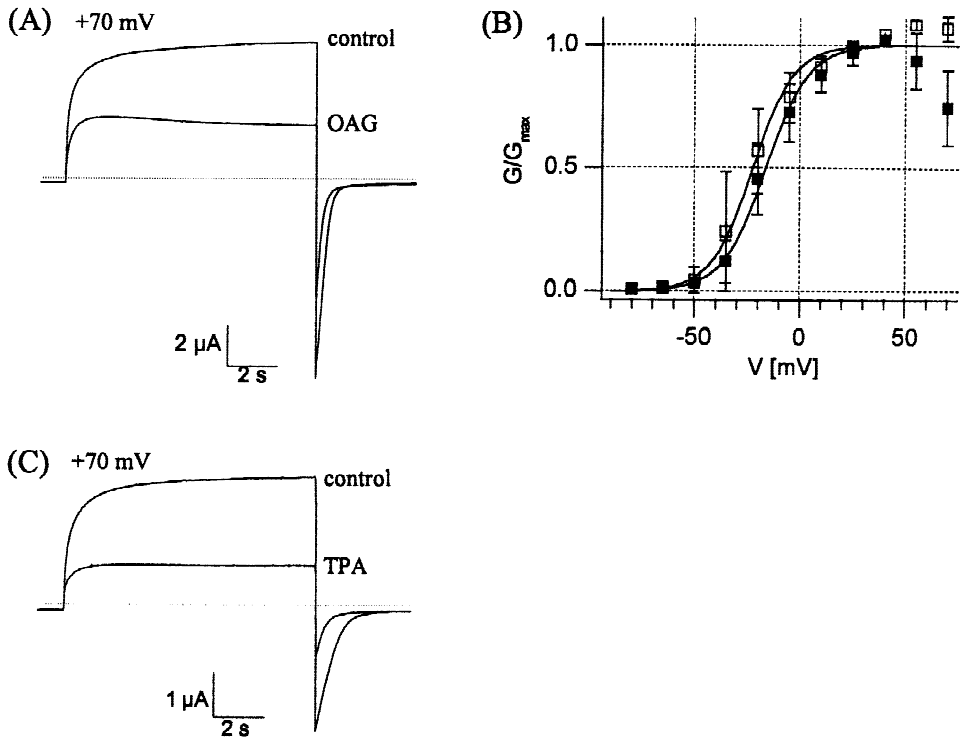


**Fig. 4.** Effect of OAG on the voltage-dependent activation and inactivation of rCx46-hemichannels. (*A*) Current-relaxations were recorded after a voltage step to +70 mV prior and 45 min after addition of 200 µM OAG to the bath as indicated. (*B*) Normalized G(*V*) curves and the corresponding fits with a simple Boltzmann function (solid lines) were determined in the absence (□, $n = 10$) and in the presence of 200 µM OAG (■, $n = 10$). (*C*) The current response to a voltage pulse of +70 mV prior and 25 min after addition of 1 nM TPA to the bath is shown. In this figure the bath solutions contained 0.25% DMSO.

tude and caused inactivation in the absence of spontaneously occurring inactivation. To study whether the OAG-induced current decrease is also based on a change in the voltage-dependent steady-state activation of the hemichannels, the *G*(*V*) curves were determined in the absence and presence of OAG. As for the studies with external $Ca^{2+}$ and protons, the control data were obtained from oocytes which did not show current inactivation at the test potential +70 mV in the presence of the corresponding control bath solution. Figure 4*B* illustrates that the *G*(*V*) curves below +40 mV were similar in the absence and presence of OAG. However, the *G*(*V*) curve for OAG-treated oocytes declined above +50 mV revealing the OAG-induced inactivation of rCx46. Statistically significant differences of the two parameters *z* and $V_{1/2}$ between control condition with 0.25% DMSO and bath solution containing 0.25% DMSO and 200 µM OAG were not found (Table). The half-activation voltage and the number of equivalent gating charges were about −20 mV and 2.5, respectively. The results suggest that the effect of OAG on the macroscopic conductance is not based on a change in the voltage threshold for activation.

## Discussion

Here, we showed that rCx46-hemichannels are differentially regulated by activation of PKC, external pH or pCa. The hemichannels undergo inactivation at low external pH or pCa or by PKC activation. Low external pH or pCa additionally stabilized the closed hemichannel state. As a result, hemichannel activation required higher depolarized potentials at high external $Ca^{2+}$ or $H^+$ concentration.

So far, the existence of active hemichannels in the native tissue was not considered because active connexons are thought to inevitably lead to cell death. However, recent studies reported that hemichannels can be also activated in native tissues such as fiber cells of mammalian lens, catfish and skate retina (DeVries & Schwarz, 1992; Malchow, Qian & Ripps, 1994; Eckert, Donaldson & Kistler, 1998). If opening/closing of hemichannels can still occur in vivo, then the cell must have developed mechanisms to keep the hemichannel in the closed state but the corresponding gap junction channel in the open state. One potential regulator might be external $Ca^{2+}$. The sensitivity of rCx46-hemichannels but insusceptibility of the rCx46-gap junction channels to external $Ca^{2+}$ in the physiological range (Fig. 2; Ebihara & Steiner, 1993) point to external $Ca^{2+}$ as a very likely candidate. Since the core and the cortex of the lens have different pH (Bassnet & Duncan, 1985), external protons may also regulate the hemichannel activity. Indeed, we observed that low external pH influenced the voltage-

dependent steady-state activation of the rCx46-hemichannels in a similar way as external $Ca^{2+}$ ions did (Figs. 2 and 3). However, the hemichannels were not sensitive to physiological pH but only to nonphysiological low pH (pH 6.0). Thus, external $Ca^{2+}$ rather than external protons may regulate the rCx46-hemichannels in the native tissue keeping them in the closed channel state.

In addition, phosphorylation/dephosphorylation processes are probably involved in controlling the rCx46-hemichannel activity (Fig. 4; Ngezahayo et al., 1998). The sensitivity of rCx46-connexons towards PKC inhibition (Ngezahayo et al., 1998) and PKC activation by the effectors OAG and TPA (Fig. 4) corresponds with the observation that rCx46 is a phosphoprotein (Berthoud et al., 1997). However, neither the phosphorylation sites in rCx46 nor the involved kinases have been yet identified. PKC- and protein-kinase-A-dependent phosphorylation sites were found in the C-terminus and in the intracellular loop of the lens connexin Cx56 from chicken (Berthoud et al., 1997). PKC-activation also caused a decrease in the Cx56-gap junction channel conductance (Berthoud et al., 1994). Since the amino acid sequences of rCx46 and Cx56 are highly homologous (62% identity), rCx46 might contain phosphorylation sites equivalent to that of Cx56.

The rCx46-hemichannels activated upon depolarization (Figs. 1–4; Ebihara & Steiner, 1993). Ebihara and Steiner (1993) suggested a sequential three-state model consisting of two closed states ($C_1$ and $C_2$) and one open hemichannel state ($O$) to account for the dependence of the activation time course on the holding voltage. We demonstrated that after hemichannel activation the rCx46-connexons occasionally inactivated when the highly depolarized voltage ($\geq$+55 mV) was maintained for several seconds (Fig. 1*B*). Considering this observation, we propose to extend the three-state model from Ebihara and Steiner (1993) to a kinetic scheme with at least four different channel states as given by the following state diagram:

$$C_1 \leftrightarrow C_2 \underset{fast}{\leftrightarrow} O \underset{very\ fast}{\overset{slow}{\rightleftarrows}} I$$

where $C_1$ and $C_2$ are the closed states (Ebihara & Steiner, 1993), $O$ is the open state, and $I$ represents the inactivated state. The probability that the hemichannels enter the open or the inactivated state increases with depolarization. In contrast, the closed states are stabilized at hyperpolarized voltages. As a result, the hemichannels return from the open or the inactivated state to the closed state upon repolarization. The fast rise of the outward current at e.g., +70 mV reflects the rapid transition from the closed states $C$ to the open state $O$ while the succeeding current decay describes the slow transition from $O$ to $I$ (Fig. 1*B*). The inactivation of rCx46 hemichannels seems to be voltage-dependent because spontaneously occurring inactivation was only observed at voltages >+50 mV rather than at every hemichannel-activating voltage pulse (Fig. 1*B*). Since the inactivation behavior was not reflected by the instantaneous tail current amplitude during repolarization (Fig. 1*B–D*), the recovery from inactivation must occur faster (<2 msec) than hemichannel deactivation. Further, we can conclude that the hemichannels very likely pass the open state in returning from the inactivated state to one of the closed states ($I \rightarrow O \rightarrow C$) rather than enter directly from $I$ to $C$ ($I \rightarrow C$).

Elevation of both, the external $Ca^{2+}$ and $H^+$ concentration, altered the hemichannel gating in a similar manner. The voltage threshold for channel activation was shifted to depolarizing potentials resulting in a decrease in hemichannel conductance (Figs. 2 and 3). Additionally, both cations may influence the permeation of rCx46-hemichannels. In comparison, external acidification altered both permeation and gating of the rat skeletal muscle $Na^+$ channel (Bénitah et al., 1997) but only the gating of the cloned plant $K^+$ channel KAT1 (Hedrich et al., 1995). In contrast to external $Ca^{2+}$ and $H^+$, PKC-dependent regulation of hemichannel activity was not related to a change in the voltage dependence of the rCx46-hemichannel activation (Fig. 4*B*). Ebihara and Steiner (1993) suggested that the $Ca^{2+}$-induced shift in voltage-dependent hemichannel activation may be based on an interaction of $Ca^{2+}$ with negatively charged amino acid residues of rCx46. Because of the similarity between the $Ca^{2+}$ and $H^+$ effect, external protons and $Ca^{2+}$ may interact with the same binding site at the channel protein. This site may be located in the external vestibule of the pore because it would easily account for the insensitivity of gap junction channel to physiological concentration of $Ca^{2+}$ (about 2 mM; Ebihara & Steiner, 1993). Then, the tight coupling of opposed hemichannels would abolish the free access of external $H^+$ and $Ca^{2+}$ to the binding site.

In addition, the PKC-activators TPA and OAG, a high external $Ca^{2+}$ or $H^+$ concentration induced inactivation of the rCx46-hemichannel. In contrast to the extracellular $Ca^{2+}$ or $H^+$ effect on the voltage-dependent activation (*see* paragraph above; Figs. 2 and 3), the voltage dependence of the inactivation, however, seems to be unaltered. The spontaneously occurring inactivation (Fig. 1*B*) as well as the $Ca^{2+}$-, $H^+$-, TPA- and OAG-induced inactivation (Figs. 2–4) always became visible above +50 mV. Recent studies on the Cx43-formed gap junction channel provided evidence that the C-terminus of the Cx43 likely plugs the permeation pathway causing the closure of the gap junction channels at a low intracellular pH (Ek-Vitorin et al., 1996; Morley et al., 1996). In similarity, the N-type inactivation of the voltage-gated *Shaker* potassium channels is based on the N-terminus that voltage independently moves into the

open pore of the potassium channel and blocks it (Hoshi, Zagotta & Aldrich, 1990). Considering the fast recovery from rCx46-hemichannel inactivation, it can be speculated that the inactivation of rCx46-connexons may be related to a comparable mechanism such as the C-terminus-caused occlusion of the channel pore. The incomplete inactivation behavior of rCx46-hemichannels and the fast recovery from inactivation would reflect a low affinity between the C-terminal inactivation ball and the receptor near the pore. As previously shown for the *Shaker* channels (Hoshi et al., 1990; Toro et al., 1994), the affinity between the ball and the receptor depends on their electrostatic attraction. Phosphorylation of the rCx46-hemichannel, external $Ca^{2+}$ or $H^+$ could directly or indirectly increase the electrostatic attraction between the C-terminal inactivation ball and its receptor, and in turn potentiate the inactivation behavior of rCx46-hemichannels.

In further studies, molecular biological and electrophysiological approaches will be combined to reveal the putative phosphorylation and protonation sites of rCx46 and the molecular mechanisms of hemichannel inactivation. The implication of the C-terminus in rCx46-hemichannel inactivation will be thoroughly examined.

The authors would like to thank Dr. I. Dreger and C. Weigt for technical assistance. This work was supported by the Deutsche Forschungsgemeinschaft (Ko 626/8-1).

## References

Baldo, G.J., Mathias R.T. 1992. Spatial variations in membrane properties in the rat lens. *Biophys. J.* **63:**518–529

Bassnet, S., Duncan, G. 1985. Direct measurement of pH in the rat lens by ion-sensitive microelectrodes. *Exp. Eye Res.* **40:**585–590

Bénitah, J.-P., Balser, J.R., Marban, E., Tomaselli, G.F. 1997. Proton inhibition of sodium channels: mechanism of gating shifts and reduced conductance. *J. Membrane Biol.* **155:**121–131

Berthoud, V.M., Westphale, E.M., Cook, A.J., Katar, M., Beyer, E.C. 1994. Expression and regulation of Cx56 chicken lens cultures. *Mol. Biol. Cell* **5:**1902*a*

Berthoud, V.M., Beyer, E.C., Kurata, W.E., Lau, A.F., Lampe, P.D. 1997. The gap-junction protein connexin 56 is phosphorylated in the intracellular loop and the carboxy-terminal region. *Eur. J. Biochem.* **244:**89–97

Bruzzone, R., White, T.W., Paul, D.L. 1996. Connections with connexins: the molecular basis of direct intercellular signaling. *Eur. J. Biochem.* **238:**1–27

Davey, P., Barza, M., Peckman, C. 1987. Spontaneous inhibition of bacterial growth in experimental gram-negative endophthalmitis. *Invest. Ophthalmol. Vis. Sci.* **28:**867–873

DeVries, S.H., Schwarz, B.A. 1992. Hemi-gap-junction channels in solitary horizontal cells of the catfish retina. *J. Physiol.* **445:**201–230

Ebihara, L., Steiner, E. 1993. Properties of a nonjunctional current expressed from a rat connexin46 cDNA in *Xenopus* oocytes. *J. Gen. Physiol.* **102:**59–74

Ebihara, L., Berthoud, V.M., Beyer, E.C. 1995. Distinct behavior of Connexin56 and Connexin46 gap junctional channels can be predicted from the behavior of their hemi-gap-junctional channels. *Biophys. J.* **68:**1796–1803

Eckert, R., Donaldson, P.J., Kistler, J. 1998. Gap junction hemichannels in fiber cells of the mammalian lens. *In:* Gap Junctions, R. Werner, editor. pp. 168–172. IOS Press Amsterdam, Berlin, Oxford, Tokyo, Washington, DC

Ek, J.F., Delmar, M.M., Perzova, R., Taffet, S.M. 1994. Role of histidine 95 on pH gating of the cardiac gap junction protein connexin43. *Circ. Res.* **74:**1058–1064

Ek-Vitorin, J., Calero, G., Morley, G.E., Coombs, W., Taffet, S.M., Delmar, M. 1996. pH regulation of connexin43: molecular analysis of the gating particle. *Biophys. J.* **71:**1273–1284

Gupta, V.K., Berthoud, V.M., Atal, N., Jarillo, J.A., Barrio, L.C., Beyer, E.C. 1994. Bovine Connexin44, a lens gap junction protein: molecular cloning, immunologic characterization, and functional expression. *Inv. Ophthalmol. Vis. Sci.* **35:**3747–3758

Hedrich, R., Moran, O., Conti, F., Busch, H., Becker, D., Gambale, F., Dreyer, I., Kuch, A., Neuwinger, K., Palme, K. 1995. Inward rectifier potassium channels in plants differ from their animal counterparts in response to voltage and channel modulators. *Europ. Biophys. J.* **24:**107–115

Hoshi, T., Zagotta, W.N., Aldrich, R.W. 1990. Biophysical and molecular mechanisms of *Shaker* potassium channel inactivation. *Science* **250:**533–538

Lin, J.S., Eckert, R., Kistler, J., Donaldson, P. 1998. Spatial differences in gap junction gating in the lens are a consequence of connexin cleavage. *Eur. J. Cell Biol.* **76:**246–250

Malchow, R.P., Qian, H., Ripps, H. 1994. A novel action of quinine and quinidine on the membrane conductance of neurons from the vertebrate retina. *J. Gen. Physiol.* **104:**1039–1055

Mathias, R.T., Riquelme, G., Rae, J.L. 1991. Cell to cell communication and pH in the frog lens. *J. Gen Physiol.* **98:**1085–1103

Mathias, R.T. Rae, J.E., Baldo, G.J. 1997. Physiological properties of the normal lens. *Physiol. Rev.* **77:**21–50

Morley, G.E., Taffet, S.M., Delmar, M. 1996. Intramolecular interactions mediate pH regulation of connexin43 channels. *Biophys. J.* **70:**1294–1302

Ngezahayo, A., Zeilinger, C., Todt I., Marten, I., Kolb, H.-A. 1998. Inactivation of expressed and conducting Cx46 hemichannels by phosphorylation. *Pfluegers Arch.* **436:**627–629

Paul, D.L., Ebihara, L., Takemoto, L.J., Swenson, K.I., Goodenough, D.A. 1991. Connexin46, a novel gap junction protein, induces voltage-gated currents in nonjunctional plasma membrane of *Xenopus* oocytes. *J. Cell Biol.* **115:**1077–1089

Rup, D.M., Veenstra, R.D., Wang, H.-Z., Brink, P.R., Beyer, E.C. 1993. Chick connexin-56, a novel lens gap junction protein. *J. Biol. Chem.* **268:**706–712

Toro, L., Ottolia, M., Stefani, E., Latorre, R. 1994. Structural determinants in the interaction of *Shaker* inactivating peptide and a $Ca^{2+}$-activated $K^+$ channel. *Biochem.* **33:**7220–7228